Phys. JETP 20, 1307 (1965)].

[2]A. I. Nikishov and V. I. Ritus, Zh. Eksp. Teor. Fiz. 50, 255 (1966) [Sov. Phys. JETP 23, 168 (1966)].

[3]A. M. Perelomov, V. S. Popov, M. V. Tetent'ev, Zh. Eksp. Teor. Fiz. 50, 1393 (1966) [Sov. Phys. JETP 23, 924 (1966)].

[4]A. M. Perelomov, V. S. Popov, and M. V. Terent'ev, Zh. Eksp. Teor. Fiz. 51, 309 (1966) [Sov. Phys. JETP 24, 207 (1967)].

[5]N. L. Manakov and L. P. Rapoport, Zh. Eksp. Teor. Fiz. 69, 842 (1975) [Sov. Phys. JETP 42, 430 (1975)].

[6]I. J. Berson, J. Phys. B8, 3078 (1975).

[7]Ya. B. Zel'dovich, N. L. Manakov, and L. P. Rapoport, Usp. Fiz. Nauk 117, 569 (1975) [Sov. Phys. Usp. 18, 920 (1975)].

[8]N. L. Manakov, M. A. Preobrazhenskiĭ, L. P. Rapoport, and A. F. Faĭnshteĭn, Zh. Eksp. Teor. Fiz. 75, 1243 (1978) [Sov. Phys. JETP 48, 626 (1978)].

[9]Ya. B. Zel'dovich, Usp. Fiz. Nauk 110, 139 (1973) [Sov. Phys. Usp. 16, 427 (1973)].

[10]N. L. Mamakov and A. G. Faĭnshteĭn, Dokl. Akad. Nauk SSSR 244, 567 (1979) [Sov. Phys. Doklady 24, 41 (1979)].

[11]A. I. Baz', Ya. B. Zel'dovich, and A. M. Perelomov, Rasseyanie, reaktsii i raspady v nerelyativistskoĭ kvantovoĭ mek-

hanike (Scattering, reactions, and decays in nonrelavistic quantum mechanics), Nauka, 1971.

[12]Yu. N. Demkov and V. N. Ostrovskiĭ, Metod potentsialov nulevogo radiusa v atomnoĭ fizike (The zero-range potential method in atomic physics), izd. LGU (Leningrad), 1975.

[13]L. D. Landau and E. M. Lifshits, Teoriya polya (Field theory), Nauka, 1973 (Engl. Transl. Pergamon, Oxford, New Yrok, 1975).

[14]I. N. Arutyunyan and G. A. Askar'yan, Pis'ma v Zh. Eksp. Teor. Fiz. 12, 378 (1970) [JETP Lett. 12, 259 (1970)].

[15]A. I. Nikishov, Zh. Eksp. Teor. Fiz. 62, 562 (1972) [Sov. Phys. JETP 35, 298 (1972)].

[16]R. V. Ambartsumyan, G. I. Bekov, V. S. Letokhov, and V. I. Mishin, Pis'ma v Zh. Eksp. Teor. Fiz. 21, 595 (1975) [JETP Lett. 21, 279 (1975)]; G. I. Bekov, V. S. Letokhov, O. I. Matveev, and V. I. Mishin, Zh. Eksp. Teor. Fiz. 75, 1052 (1978) [Sov. Phys. JETP 48, 1052 (1978)].

[17]L. P. Rapoport, B. A. Zon, and N. L. Manakov, Teoriya mnogofotonnykh protesessov v atomakh (Theory of multiphoton processes in atoms), Atomizdat, 1978.

Translated by E. Brunner

Interference of synchrotron radiation

M. M. Nikitin, A. F. Medvedev, M. B. Moiseev, and V. Ya. Épp

Nuclear Physics Research Institute at the Tomsk Polytechnic Institute

Interference of synchrotron radiation of relativistic electrons, which is synchronized consecutively by the particle beam itself at two points separated by a long straight gap is investigated. The spectral and polarization-angular characteristics of the radiation are studied. Satisfactory agreement between theory and experiment is obtained. It is shown that the interference of synchrotron radiation in installations in which the magnetic field drops off sharply in the straight gap, and in which the electron beam has a small variance of the angular spread of the particles, can be of independent significance, on top of synchrotron and wiggler radiation, for the solution of many scientific and applied problems.

PACS numbers: 41.70. + t

INTRODUCTION

In experiments[1,2] on the properties of wiggler radiation (WR) of relativistic electrons in a magnetic wiggler mounted in one of the straight sections of a synchrotron, it was noted that the synchrotron radiation (R) of the particles in the stray magnetic field at the entrance and exit of the straight gap of the accelerator constitute an undersirable "background" in the observation of the polarization-angular characteristics of the WR (especially at high electron energies). A more detailed investigation of this background has revealed the effect of interference of synchrotron radiation[3] (ISR) in the region where the radiation of the electrons from the far and near ends of the straight gap of the synchrotron overlap. The radiation from these ends of the gap can be represented as the radiation of two quasi-pointlike SR sources the distance between which is L (comparable with the length of the gap), synchronized successively by the electron itself, which moves with velocity $v = \beta c$ (c is the speed of light).

The properties of SR are particles moving along a closed circle were investigated in sufficient detail both theoretically[4,5] and experimentally.[6,7] It turned out, however, that the radiation of the electrons in the direction of the straight gap has certain singularities connected with the interference of the radiation. No attention was paid to this circumstance before, and this question remained uninvestigated. Interest in ISR is raised also by the fact that at the present time more and more attention is being paid to the use of straight gaps of electron synchrotrons and storage rings in order to place in them special magnetic systems (e.g., wigglers), and to generate in these systems, by a relativistic electron beam, radiation that can be used together with SR to solve a large group of scientific and applied problems. It is clear that in such investigations the ISR must also be taken into account. This article presents the results of an investigation of the ISR phenomenon.

1. EXPERIMENTAL PROCEDURE AND SETUP

The ISR was experimentally investigated with the 1.5-GeV "Sirius" electron synchrotron,[8] whose straight

gaps were 1.57 m long. The electron radiation was extracted from the vacuum chamber of the synchrotron through a glass illuminator whose axis coincided with the axis of the straight gap of the accelerator. In the path of the SR beam were placed an objective, in the focal plane of which it was possible to observe the pattern of the angular distribution of the radiation in the optical region of the spectrum, a polarizer capable of eliminating the linear polarization components, and an interference light filter. A pinpoint diaphragm, which passed radiation with an angle aperture $\Delta\Omega \approx 49.5 \cdot 10^{-10}$ sr was placed in the focal plane of the objective and used to measure the spectrum and the angular distribution of the IRS intensity. The recording element was a photomultiplier. The resolution of the radiation polarization intercomponent was the same as used in Refs. 1-4 for SR and WR. This resolution is more convenient from the point of view of experimental verification, inasmuch as in this case the orientation of the components of the electric field intensity vector of the radiation no longer depend on the radiation direction. This makes it possible to resolve the entire radiated energy of the ultrarelativistic electron into two components with polarization planes perpendicular (σ) and parallel (π) to the magnetic field.

The pattern of the radiation of a relativistic electron in the direction of the axis of the straight gap of the synchrotron is shown in Fig. 1. The electron radiation in the far (A) and near (B) end of the gap is synchronized by the electron itself. Consequently the field of the radiation from the point B is delayed relative to the point A by a time

$$\Delta t = t_e - t_\lambda,$$

where $t_e = l_e / \beta c$ is the time of electron motion between the radiation points, $l_e = L + 2R(\varphi' - \sin\varphi')$ is the electron-trajectory length, R is the radius of the curved trajectory of the electron in a magnetic field H at the radiation points, $t_\lambda = l_\lambda / c$ is the time of propagation of the wave between the radiation points, $l_\lambda \simeq L\cos\theta\cos\varphi$, and θ and φ are the radiation observation angles. In the region where the SR rays overlap we have $2\varphi' \simeq \gamma^{-1}$, where γ is the relativistic factor.

When ISR is observed at a wavelength λ, the order of the interference is equal to $m = \Delta t c / \lambda$. The maxima of the equalslope lines correspond to the values $m = 0, 1, 2, \ldots$, and the minima to $m = 0.5; 1.5; \ldots$. At any given value of m, the equal-phase surface of the radiation field in the interference pattern is located on a circle of radius
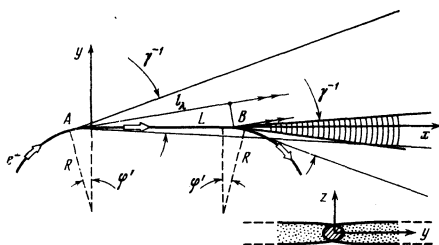
FIG. 1. Motion and radiation of electron in a straight gap (definition of notation).

$$\delta = (\theta^2 + \varphi^2)^{1/2} = 2^{1/2} \left[\frac{m\lambda}{L} - \frac{1}{\beta(1+\beta)\gamma^2} - \frac{2R(\varphi' - \sin\varphi')}{\beta L} \right]^{1/2}. \quad (1)$$

This expression can also be used to estimate the ultra-relativistic-electron energy corresponding to observation of a given order of interference at a wavelength λ and at an angle δ_m. Recognizing that $R\varphi' \ll L$, we have

$$\gamma \simeq [2(m\lambda/L - \delta_m^2/2)]^{-1/2}. \quad (2)$$

In the measurements of the ISR spectrum, the pinpoint diaphragm was placed at the center of the region of the overlap of the radiation from the far and near ends of the straight gap. The long duration of the acceleration cycle (44 msec) made it possible to measure the radiation intensity of quasi-monoenergetic electron ($\Delta E \approx 0.049$ MeV) with a minimum energy step of ~0.17 MeV. The measurement assembly automatically carried out normalization to the number of accelerated particles in each acceleration cycle, with the background subtracted, and averaging of the results of the measurements at each point over 50 cycles of electron acceleration. The relative measurement error did not exceed 5%.

We note that the ISR spectrum was obtained by a procedure developed in the investigation of WR, i.e., the spectrum was "extended" so to speak through the fixed observation wavelength λ_f. The following dependence of the number of radiated photons on the electron energy E at the wavelength λ_f yields the radiation spectrum, since the energy of the electrons is connected with the reduced number of the harmonic ν of the radiation by the relation

$$\nu = 2\pi R (m_0 c^2)^3 E^{-3} / 3\lambda_f. \quad (3)$$

Consequently, the IRS spectra obtained in this paper are universal in character, inasmuch as at a certain constant electron energy the radiation wavelength is determined by the value of ν:

$$\lambda = 2\pi R \nu^{-1} / 3\gamma^3. \quad (4)$$

Thus, to estimate experimentally the values of ν and λ by means of expressions (3) and (4) it is necessary to measure the effective radius of the electron orbit in the region of the radiation points that produce the interference pattern. In addition, knowing the value of R, we can estimate also the influence of the inhomogeneous magnetic field at the radiation points on the visibility factor of the interference pattern, i.e., the third term in (1) can be neglected under the condition

$$R \ll {}^3/_2 \beta L\gamma.$$

2. DETERMINATION OF R AT THE PARTICLE RADIATION POINTS

The equilibrium radius R_S, of the moving electron in the turning magnetic field of the cyclic accelerator is usually known quite accurately. In our case, on the other hand, we register the radiation of the electrons at some azimuthal point of the stray magnetic field at the edges of the turning magnets of the accelerator. The problem is thus to determine R (or H) at the radiation point, knowing only the particle energy at the instant of measurement, and without determining the location of the radiation point relative, e.g., to the edge of the magnet. This problem could be solved with

the aid of the universal SR spectrum, after first verifying the agreement between its theoretical description and experiment. In turn, measurement of the SR spectrum in a very wide range by any traditional method is practically impossible[9] (it is known that the SR spectrum extends from radio waves to x rays).

The gist of the proposed method of measuring the universal SR spectrum is that one scans in the experiment not the radiation wavelength λ at a certain constant electron energy, but the critical SR wavelength λ_s by varying the energy of the particles at a fixed observation wavelength λ_f. The investigated spectral band is thus expanded by hundreds of times and a high experimental accuracy is attained. The measurement range is limited on the one side by the maximum particle energy attainable in the given accelerator, and on the other side by the possibility of recording very weak SR intensities. Thus, the described method made it possible to investigate experimentally, for the first time ever, the universal spectral function $\varphi_i(y)$ of SR in practically its entire interval ($y \approx 10^{-4} - 50$, where $y = \lambda_s \lambda^{-1}$).

The experimental results are shown in Fig. 2. The observation was carried out at a wavelength $\lambda_f = 500$ nm ($\Delta\lambda = 10$ nm) on the curved section of the particle trajectory with an equilibrium radius $R_s = 423$ cm. We measured directly the number of N of radiated photons with wavelength λ_f. This number is directly proportional to the quantity

$$N_{k_i}(\lambda) = 1.256 \cdot 10^{10} k_1 \gamma \varphi_i(y) \left[\frac{\text{photon}}{\Delta\lambda \cdot \text{sec} \cdot \text{mA} \cdot \text{mrad}} \right]$$

(here $k_1 = \lambda^{-1}\Delta\lambda$), passing through the slit diaphragm integrally over the vertical observation angle, and ~1 mrad in the horizontal direction. The electron-energy scanning and the general measurement technique remained the same as in the investigation of the IRS spectrum. The theoretical curves of Fig. 2 were plotted in accordance with the formulas of Ref. 4.

The values of y were determined from the relation

$$y = 4\pi R_s / 3\lambda_f \gamma^3.$$

The maxima $\varphi_0(y^{-1})$ and $\varphi_2(y^{-1})$ of the experimental distribution were normalized to the maxima of their theoretical values. As seen from Fig. 2, the positions
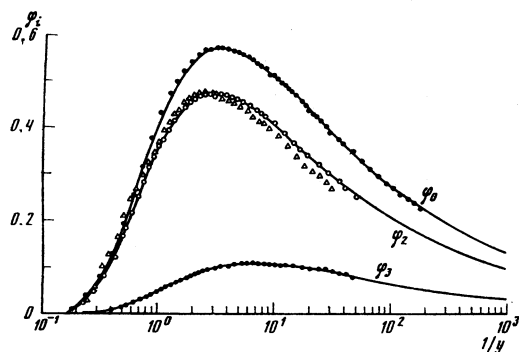
FIG. 2. Universal spectra of the various components of angle-itegrated observed SR: φ_2) σ components, φ_3) π components, φ_0) $\sigma + \pi$ components, solid curves—theory, $\triangle$) experimental spectrum of σ component at the center of the SR cone.

of the experimental maxima, the relations between the experimental distributions $\varphi_2(y^{-1})$ and $\varphi_3(y^{-1})$, and the general behavior of the curves in the experiment agrees well with the theoretical calculation. The same figure shows the universal spectrum of the σ components of the SR, measured on the axis of a radiation cone in a solid angle 1.4×10^{-6} sr, the maximum of which was equated to the maximum of the function $\varphi_2(y^{-1})$. It is seen that the maximum of this distribution is noticeably shifted towards the short-wave region of the SR relative to the maximum of the spectrum integrated over the angles. Incidentally, a similar shift was noted also in the investigation of WR.[2]

Thus, recognizing that the universal spectral SR function is measured in experiment agree well with the theory, it suffices to determine the electron energy E_m corresponding to the maximum of the electron distribution, e.g., φ_2 in accordance with the procedure described here for a certain wavelength λ_f at the investigated radiation point, and then determine R (or H) at this point, knowing the position of the maximum and the theoretical distribution φ_2, using the following derived relations:

$$H (\text{kOe}) \approx 5.5913 \cdot \lambda_f \, (\text{cm}) \cdot E_m^{-2} \, (\text{MeV}), \tag{5}$$

$$R \, (\text{cm}) \approx 0.5963 \cdot \lambda_f \, (\text{cm}) \cdot E_m^3 \, (\text{MeV}). \tag{6}$$

An estimate of the average radius of the curved electron trajectory at quasipoints located on the ends of the linear gap symmetrically with respect to its center and producing the ISR was obtained by the procedure described above. It turned out that $R \approx 69$ m and $H \approx 315$ Oe.

3. ANGULAR DISTRIBUTION OF ISR

The general picture of the angular distribution of the ISR was photographed. An electrodynamic shutter of the impact type was placed on the path of the ISR beam and was turned on at specified instants of the particle acceleration cycle with exposure ~200 μsec. Photographs of the interference patterns of the ISR at a wavelength 582 nm for different electron energies and for both components of the linear polarization are shown in Fig. 3. It is seen that in the region of the overlap of the SR from the far (right) and near (left) ends of the gap there is interference between radiation of not only the σ but also the π component of the SR. The narrowing of the vertical-angular distribution of the SR towards the center (this is particularly clearly seen for the π component) indicates that what is actually observed is interference of photons from trajectory points located in the stray field on both ends of the magnets, and not a simple superposition of patterns from different sections of the stray field. Thus, on photograph 4a (Fig. 3), at the center of the picture, is localized the order of interference $m = 0.43$—a growing maximum of zeroth order, and next, with increasing vertical observation angle, the same photograph shows the maxima of the first order of interference. The broadening of the maxima on the photographs 4a and 4b in the radial direction is due to the influence of the large angle spread of the electrons in the beam as a result of the buildup of radial betatron oscillations
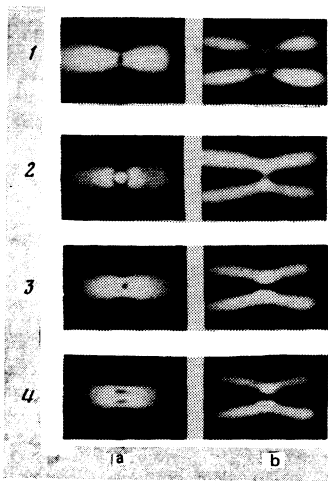
FIG. 3. Interference patterns of σ and π components of radiation polarization (a and b, respectively) at particle energies 433 (1), 542 (2), 686 (3), 903 MeV (4).

due to quantum fluctuations of the SR at high particle energies. On the remaining photographs of the σ component (1a–3a) one observes at the center of the picture the minima and maxima of the ISR of the given wavelength as functions of the electron energy. Corresponding changes take place also in the π component of the radiation (photographs 1b–4b of Fig. 3).

More details on the ISR are obtained by measuring the vertical-angular distribution of the radiation intensity with the aid of a scanning pinpoint diaphragm, using the procedure described above. The experiment was performed at an angle $\varphi = 0$ at the same observation wavelength and the same electron energy as used to photograph the general interference pattern 4a and 4b of Fig. 3. The result of the experiment is shown in Fig. 4. The intensity of the radiation of the π component was normalized to the maximum of the σ component of the ISR. The overall angular dimension of the radiation corresponds to the vertical-angular distribution of the SR of the electrons at the radiation
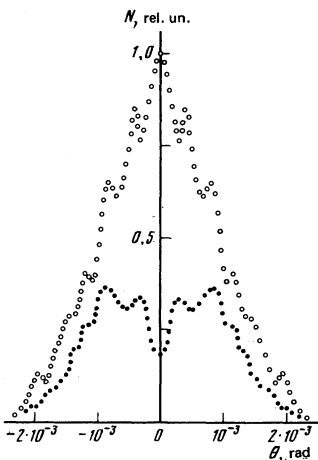
FIG. 4. Experimental vertical-angular distribution of the number of σ- and π-component radiation-polarization photons (light and dark circles, respectively).

points at the given wavelength and particle energy.

It is seen from the figure that at the center of the σ component $(\theta = 0)$ there is a growing maximum of the zeroth order of interference, and with increasing observation angle one can see next the maxima of the first, second, etc. orders. The nonzero minimum of the π component at the angle $\theta = 0$, and also the "smearing" of the interference maxima on both curves, are attributed to the influence mainly of the angle scatter of the particles in the beam. We note that the angular positions of the interference maxima in the σ and π components of the ISR do not coincide, and the angular dimension of the maxima is of the order of 10^{-4} rad. In contrast to Fig. 4, Fig. 3 (4a, 4b) shows more clearly the minima between the maxima of the first and zeroth order, and hardly show the maxima of the next interference orders in the pattern, owing to the high contrast and the low sensitivity of the photographic material employed.

The average distance between the radiation points can be estimated (with allowance for the fact that $R\varphi' \ll L$) by measuring the angular position (δ_m and δ_{m+k}, where k is the number of rings between the rings of radius δ_m and δ_{m+k}) of the maxima in the interference pattern:

$$L \approx 2k\lambda/(\delta_{m+k}^2 - \delta_m^2). \tag{7}$$

It was found that $L \approx 135$ cm, i.e., the radiation points are located in a magnetic field that falls off in the linear gap from the main magnets of the synchrotron, and is located ~11 cm away from the edges of the magnets.

Thus, the region of the radiation points on the curved section of the particle trajectory ($R\gamma^{-1} \approx 5$–10 cm) is located in a smoothly inhomogeneous magnetic field. In the gap between the interfering regions of the radiation points there is no magnetic field. The radiation from the remaining part of the electron orbit does not land in the straight gap, all the more if the field in that section is stronger than the field in the regions of the points A and B (see Fig. 1). When the radiation is observed at low frequencies, as in our case, we can make a certain assumption that corresponds approximately to the experimental conditions. We take a certain mean value of the magnetic field in the region of the radiation points, in which the electron moves on a curved trajectory with an effective radius R, the measurement of which was described above. We can then obtain in the ultrarelativistic approximation, using standard methods of classical electrodynamics,[4,5,10] the spectral-angular distribution of the radiation energy of the σ component of the ISR in the vertical plane xz ($\varphi = 0$) in which the experiment is performed:

$$dE_\sigma/d\omega d\Omega = W[(2\pi/3)I_{\frac{2}{3}}(p)$$
$$+ (\text{ctg }\mu + 3^{-\frac{1}{2}})K_{\frac{2}{3}}(p) - (\pi/3)T_1(p)]^2,$$
$$W = (3e^2 v^2 \gamma^2/\pi^2 c)(1+\psi^2)^2 \sin^2 \mu,$$
$$T_1(p) = \frac{2}{3}\sum_{m=1}^{\infty} \frac{(3m-1)p^{2m-2}}{2^{2m-2}\Gamma(m+\frac{1}{3})\Gamma(m+\frac{2}{3})},$$
$$\mu = (3L\gamma v/4R)(1+\psi^2), \quad p = v(1+\psi^2)^{\frac{3}{2}},$$
$$v = (\omega/\omega_0)\frac{1}{3\gamma^3}, \quad \psi = \theta\gamma,$$

$$\tag{8}$$

Nikitin *et al.*   391

where $K_{2/3}(p)$ is a modified Bessel function of fractional index, $I_{2/3}(p)$ is a Bessel function of imaginary argument, $\Gamma(x)$ is a gamma function, ω is the radiation frequency, ω_0 is the frequency of revolution of the electron in the accelerator, and ν is the reduced number of the harmonic of the radiation at the observation angle $\psi=0$. The observation angle θ is small, $\sim\gamma^{-1}$, and is chosen such that the unit vector of the radiation direction n in the coordinate system shown in Fig. 1 has the components $\{\cos\theta\cos\varphi,\ \cos\theta\sin\varphi,\ \sin\theta\}$. If we choose $L=0$, then Eq. (8) goes over into the classical expression for the SR. The presence of the factor $\sin^2\mu$ indicates that the spectrum is strongly modulated (the interference phenomenon). The modulation frequency is determined mainly by the parameter μ, and the form of the spectrum is determined by the ratio of the quantities R and L. Interference of the radiation becomes already noticeable at a gap length $L>R\gamma^{-1}$. At low frequencies, i.e., as $\gamma\to\infty$ $(p\to0)$, the spectrum along the axis of the radiation cone can be represented by the asymptotic formula

$$\frac{dE_\sigma}{d\omega\,d\Omega}=\frac{4e^2}{c[\Gamma(^1/_3)]^2}\left(\frac{\pi R}{3\lambda}\right)^{2/3}$$
$$\times\left\{1+\left[\frac{\pi L}{3^{1/6}\lambda}-\frac{6}{\pi}\Gamma\left(\frac{1}{3}\right)\left(\frac{\pi R}{3\lambda}\right)^{2/3}\right]\gamma^{-2}+O(\gamma^{-4})\right\}. \tag{9}$$

A comparison of the experimental results with calculation for the vertical-angular distribution at the center ($\varphi=0$) of the IRS was carried out for the σ component of the radiation at the wavelength $\lambda=582$ nm ($\Delta\lambda=12$ nm) at a particle energy 722 MeV (Fig. 5). The normalization was such that the areas under the experimental and theoretical curves were equal. At the center of the IRS cone ($\varphi=0$, $\theta=0$) one can see a rise in the radiation intensity of the zeroth interference order, and at the angle $\theta\approx\pm0.6\cdot10^{-3}$ rad are localized the maxima of the first order. We see that the angular distribution of the σ component in the IRS differs substantially from its known distribution in SR,[4,6,7] in which the maximum of the σ component is always localized at an angle $\theta=0$ and decreases smoothly with increasing vertical observation angle θ.

The theretical calculation was made for one electron, although in fact, of course, the radiation is produced by a beam of particles. The vertical-angular scatter of the electrons in the beam smears out somewhat the interference pattern, and this leads to a decrease in the intensity of the radiation and to a broadening of the
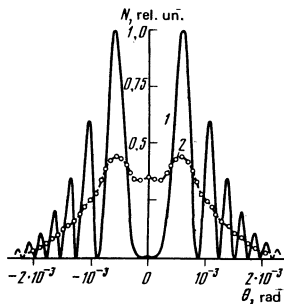
first-order interference. A certain inhomogeneity of the field at the radiation points and the angle scatter of the particles also cause the next order of interference to be weakly visible in the experiment. This explains also the rather high intensity of radiation at the center of the IRS cone relative to its theoretical value as well as the absence of zero intensity dips between the maxima in the interference pattern. The angular distribution of the ISR in Fig. 4 was obtained at a higher electron energy, at which the vertical-angular scatter of the particles is several times smaller than at 722 MeV,[6,11] therefore the interference maxima are more clearly seen on Fig. 4 than on Fig. 5. We note, however, that the general shape of the curves in Fig. 5, and in particular the angle position of the maxima are on the whole the same in the calculation and in the experiment.

4. SPECTRAL-ANGULAR DISTRIBUTION

The dependence of the radiation intensity of the σ component at the center of the interference pattern on the electron energy for two different wavelengths is shown in Fig. 6. The maxima of first-order interference are normalized to their theoretical value calculated from Eq. (8). As expected, when the observation wavelength is decreased a particular order of the interference arises at a higher electron energy. Thus, at the wavelength $\lambda_1=500$ nm ($\Delta\lambda_1=10$ nm) the orders m of the interference on the axis of the radiation cone correspond to the following particle energies: 592 ($m=2$); 333.9 ($m=3$); 290.6 MeV ($m=4$), and at the wavelength $\lambda_2=582$ nm ($\Delta\lambda_2=12$ nm) they correspond to 548.7 ($m=1$); 382.7 ($m=2$); 309.5 ($m=3$); 269.3 MeV ($m=4$); for any value of m, the ratio of the electron energy E_1 (at λ_1) to the energy E_2 (at λ_2) satisfies the condition

$$E_1/E_2=(\lambda_2/\lambda_1)^{1/2}. \tag{10}$$

From this we readily obtain

$$\Delta E=E_1-E_2=E_1(1-(\lambda_1/\lambda_2)^{1/2}). \tag{11}$$

The experimental values of ΔE turned out to be in good agreement with the calculation. Thus, in the ex-

FIG. 5. Vertical-angular distribution of the intensity of the ISR σ component (1—theory, 2—experiment).
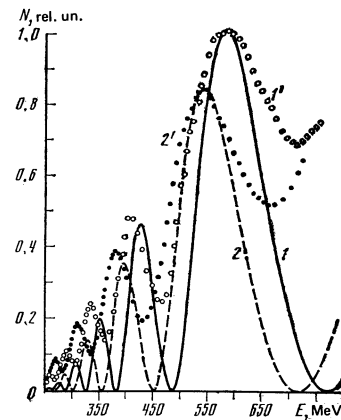
FIG. 6. Experimental (1 and 1') and theoretical (1 and 2) spectra of σ component along the ISR cone at observation wavelengths 500 (1 and 1') and 582 (2 and 2') nm.

periment $\Delta E \approx 43.3$ (at $m=1$; 30 ($m=2$); 24.4 ($m=3$); and 21.25 MeV ($m=4$). The general rise of the radiation intensity with increasing electron energy is due to the characteristic dependence of the SR intensity at a given observation wavelength at the radiation points on the particle-beam energy.[4] It is also seen from the figure that the SR from the radiation points are partially coherent with each other. Thus, at the wavelength λ_2 the visibility factor V of the interference pattern[12] is equal to 0.59 ($m=1$); 0.57 ($m=2$); 0.54 ($m=3$), etc. The value of V is substantially influenced by the angle scatter of the electrons in the beam mainly because of their betatron oscillations in the accelerator, since the angle scatter of the particles is comparable with the apex angle of the SR cone. In comparison, the influence exerted on V by the final width of the transmission of the interference light filters ($\Delta\lambda/\lambda \approx 2 \cdot 10^{-2}$) in experiment is negligible. An estimate of the coherence length of the ISR for the experimental conditions yields a value $L_{coh} \approx 0.02$ mm. At high electron energies (above 700 MeV) there is observed in the center of the IRS pattern an increase of the intensity of the zero-order interference.

A comparison of the theoretical curves with the experimental data in Fig. 6 shows that the experimental positions of the maxima of the first order of interference in the electron-energy scale agree with their calculated positions. There is also satisfactory agreement between experiment and theory for the difference in the radiation intensity at different wavelengths, but at the same interference order, and also in the value of ΔE, as mentioned above. However, in general the experimental curves lie somewhat higher than the calculated data and the experimental positions of the interference maxima are shifted from the calculated values towards lower electron energy by ~15 MeV. This can be attributed, on the one had, again to the angle scatter of the particles in the beam, which leads also to the presence of nonzero minima of the intensity in the experimental spectrum, and on the other hand to the inaccuracy with which the values of R and L used in the theoretical calculations were determined, since these values influence substantially the form of the ISR spectrum. When this is taken into account, the agreement between experiment and theory can be regarded as satisfactory.

It was impossible to perform the experiment at higher electron energies, therefore Fig. 7 shows the subsequent course of the theoretical curves of Fig. 6 in the electron-energy scale. The same radiation-intensity scale is used in Figs. 6 and 7. The cross on Fig. 7 shows the position of the first-order maximum at the wavelength 500 nm, and the circle shows the corresponding maximum for $\lambda = 582$ nm. Up to an electron energy ~3.5 GeV ($p = 0.001$) the curves are plotted in accordance with Eq. (8), and above that we used the asymptotic approximation (9). It is seen from the figure that the maxima of the zero-order interference of the given wavelengths are localized in the electron-energy region ~1.5 GeV, and the maximum at the 500 nm wavelength is located in the region of higher particle energies than the corresponding maximum at λ
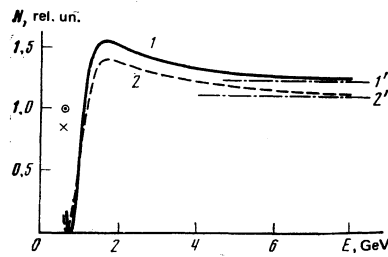
FIG. 7. Zeroth order of interference in the spectrum of the σ component along the axis of the IRS cone at observation wavelengths 500 (1) and 582 (2) nm.

$= 582$ nm. With further increase of the electron energy ($E \to \infty$) the radiation intensity decreases and approaches asymptotically the SR levels at these wavelengths (1' and 2').

At the same time, measurement of the ISR integrated over the observation angles is of interest. This was also done in accord with the procedure described above. In the focal plane of the objective, precisely at the center of the region of abrupt change of the radiation from the far and near ends of the gap, a vertical slit diaphragm was installed and restricted the radiation in the radial direction to ~0.8×10⁻³ rad without limiting the angular distribution of the ISR in the vertical direction. To compare the results of the experiments with the data of Figs. 4 and 6, the spectrum was also measured at the wavelength 582 nm. The results are shown in Fig. 8. The intensities of the 6 and π components were normalized to the same value. As seen from the figure, the degree of polarization of the ISR integrated over the vertical observation angle is determined mainly by the σ component. In the π component there are also observed weak oscillations of the intensity with increasing electron energy, and these oscillations correspond approximately to the oscillations in the σ component.

Another fact of interest is that the maxima in the component are shifted towards higher electron energies relative to their corresponding positions in the spectrum obtained exactly along the axis of the ISR cone (see Fig. 6). Thus, the maximum of the first-order interference on Fig. 8 is shifted relative to its position on Fig. 6 by ~31 MeV, that of the second order by ~7.3 MeV, and of the third by ~0.5 MeV. We note that an approximately similar behavior of the curves and shift of the maxima were observed also in the spectra of the WR.[2,13] It turned out that the ISR spectrum is somehow intermediate between the SR and WR spectra. We note
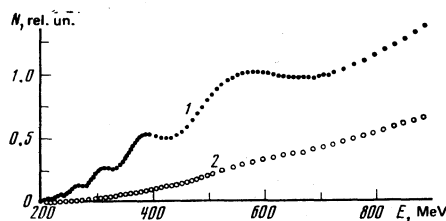
FIG. 8. Experimental spectrum of σ and π components of the ISR integrated over the vertical observation angle (curves 1 and 2, respectively).

also that in the integrated spectrum of the ISR the ratio of the intensities of the σ and π components at an electron energy 903 MeV is approximately equal to the ratio of the areas under the experimental curves of these components in the angular distribution of the ISR in Fig. 4; this indicates that the experimental results on these figures are on the whole in good agreement.

CONCLUSION

Thus, we have shown that a correlation exists between the SR of electrons at two points separated by a large gap, despite the fact that statistically the electrons radiate independently.[4,14] In installations in which the magnetic field decreases relatively rapidly in the straight gap, and the angle scatter of the electron beam has a small variance, the ISR can be of independent significance, alongside with SR and WR, in the solution of a large number of scientific and practical problems. It is obvious that in the region where the magnetic field terminates abruptly the spectrum of the radiation extends farther into the high-frequency region than the SR spectrum in the same magnet. Thus, in Ref. 13, in observations along the axis of the straight gap of the synchrotron, they succeeded in observating radiation of protons with energy ~400 GeV in the optical region of the spectrum. This uncovers new possibilities of non-destructive methods of monitoring the parameters of a proton beam.

One can expect to observe in magnetic wigglers with large magnetic fields, when the cones of the radiation from different "humps" of the trajectory of the electrons do not overlap, radiation similar to ISR from M like humps, inasmuch as the radiation in this case is also phased by the same electron. Variation of the distance between the radiation points at constant E makes it possible to observe the interference pattern in other spectral bands of the SR. Consequently, by placing in the straight gap, e.g., a magnetic wiggler designed to generate WR at a given particle energy in another spectrum interval, it is possible to regulate additionally the path difference of the SR rays over a range

$$\Delta l \approx L_w / 16\gamma^2\xi^2$$

(L_w is the wiggler length, and ξ is a parameter that characterizes the strength of the magnetic field and its influence on the form of the SR spectrum[16]), and by the same token increase the number of observable interference orders. We note that the influence of the angle scatter of the particles is largest in observation of IRS in the shorter-wavelength region, for example, in the region of the vacuum ultraviolet or soft x rays.

[1]A. N. Didenko, A. V. Kozhevnikov, A. F. Medvedev, M. M. Nikitin, and V. Ya. Épp, Zh. Eksp. Teor. Fiz. 76, 1919 (1979) [Sov. Phys. JETP 49, 973 (1979)].

[2]A. F. Medvedev, M. M. Nikitin, and V. Ya. Épp, Pis'ma v Zh. Tekh. Fiz. 5, 795 (1979) [Sov. Tech. Phys. Lett. 5, 327 (1979)].

[3]M. M. Nikitin, A. F. Medvedev, and M. B. Moiseev, ibid. 5, 843 (1979) [5, 347 (1979)].

[4]In: Sinkhrotronne izluchenie (Synchrotron Radiation), ed. by A. A. Sokolov and I. M. Ternov, Nauka, 1966.

[5]V. M. Baier, V. M. Katkov, and V. S. Fadin, Izluchenie relyativistkikh elektronv (Radiation of Relativistic Electrons), Atomizdat, 1973.

[6]O. F. Kulikova, Trudy FIAN SSSR 80, 3 (1975).

[7]A. A. Vorob'ev, M. M. Nikitin, and A. V. Kozhevnikov, At. Énerg. 29, 389 (1970).

[8]A. A. Vorob'ev, A. P. Chuchalin, A. G. Vlasov, V. N. Kuz'min, G. A. Sipaĭlov, B. A. Solntsev, G. P. Fomenko, and P. M. Shchanin, Sinkhrotron TPI na 1.5 GeV (the Tomsk Polytechnic 1.5 GeV synchrotron), Atomizdat, 1968.

[9]Sinkhrotronnoe izluchenie v issledovanii tverdykh tel (Synchrotron Radiation in Solid-State Research) (collection of translations), Mir, 1970.

[10]L. D. Landau and E. M. Lifshitz, Teoriya polya (Classical Theory of Fields), Nauka, 1973, Pergamon.

[11]A. V. Kozhevnikov, M. M. Nikitin, and A. F. Medvedev, Izv. Vyssh. Ucheb. Saved.-Fizika, No. 10, 115 (1971).

[12]M. Born and E. Wolf, Principles of Optics, Pergamon, 1970.

[13]I. M. Ternov, V. R. Khalilov, V. G. Bagrov, and M. M. Nikitin (izv. Vyssh. Ucheb Zaved., Fizika, No. 2, 5, (1980).

[14]I. A. Grishaev, I. S. Guk, A. S. Mazmanishvili, N. I. Mocheshnikov, L. V. Reprintsev, A. S. Tarasehnko, and A. M. Shenderovich, Preprint No. 70-36, Kharkov Phys. Tech. Inst., 1970.

[15]H. Bossart, J. Bosser, L. Burnod, R. Coisson, E. d'Amico, A. Hofmann, and J. Mann. Nucl. Instr. Meth. 164, 375 (1979).

[16]M. M. Nikitin and A. F. Medvedev, Zh. Tekh. Fiz. 45, 950 (1975) [Sov. Phys. Tech. Phys. 20, 600 (1975)].

Translated by J. G. Adashko